**Smart Structures and Systems**, *Vol. 28, No. 3 (2021) 305-318*
https://doi.org/10.12989/sss.2021.28.3.305


# Effect of applied electric potential and micro length scale parameters on the electroelastic analysis of three-layered shear deformable micro-shell

Yang Yang [1a], Keyong Shen*[2b], Gholamreza Ghasemian Talkhunche [3c] and Mohammad Arefi [3d]

[1] *School of Electronics and Information, Nanchang Institute of Technology, Nanchang 330044, Jiangxi, China*
[2] *School of Computer Information Engineering, Nanchang Institute of Technology, Nanchang 330044, Jiangxi, China*
[3] *Department of Solid Mechanics, University of Kashan, Kashan 87317-51167, Iran*

(*Received May 16, 2020, Revised June 14, 2021, Accepted July 8, 2021*)

**Abstract.** This paper uses higher-order shear deformation theory and modified couple stress theory (MCST) to the electroelastic results of FG micro-shell integrated with piezoelectric thin sheets subjected to electrical and mechanical loads rested on Pasternak's foundation. Third-order shear deformation theory (TSDT) is used for the description of the displacement field. Effect of micro-size is applied using MCST with the introduction of one micro-length scale parameter. Governing equations are derived based on the principle of virtual work. Micro-shell is composed of a FG micro core and two piezoelectric hollow shells. The numerical results are obtained for the simply-supported boundary conditions. Longitudinal and radial displacements are presented in terms of important parameters such as applied electric potentials, micro length scale parameter, dimensionless geometric parameters and two parameters of Pasternak's foundation.

**Keywords:** applied electric potential; axial and radial displacements; micro-length scale parameter; micro-shell; third-order shear deformation theory

## 1. Introduction

Cylindrical shells are used in various situations as important elements of mechanical engineering. This element has been analyzed by various researchers with a focus on the vibration, bending and buckling behaviors. The cylindrical shells have been analyzed by various analytical and numerical methods based on continuum mechanics that do not account the size of element on the used theory. The literature review is presented to show the importance of the present work.

Wave propagation analysis of carbon nanotubes was studied based on the nonlocal elastic shell theory by Wang and Varadan (2007). Wave propagation characteristics have been reported in terms of small-scale parameters and dimensionless geometric parameters of the problem. Effect of thermal, mechanical and electrical pre-loads was studied on the size-dependent vibration analysis of piezoelectric cylindrical nanoshells by Ke *et al*. (2014a). MCST and FSDT were used for size-dependent free vibration analysis of FG nanoshell by Tadi Beni *et al*. (2015). Navier's solution was used for numerical analysis of the problem. Free vibration characteristics were presented in terms of main parameters of the problem such as small scale parameter, in-homogeneous index, dimensionless geometric parameters such as length to radius and radius to thickness ratios.

Nonlinear buckling and post-buckling analysis of piezoelectric cylindrical nanoshell subjected to axial mechanical and electrical loads were studied by Sahmani *et al*. (2016). Surface elasticity theory was used based on Gurtin–Murdoch elasticity theory and geometrical nonlinearity was employed by von Karman relations. They concluded that an increase of surface energy and electric potential leads to an increase and decrease of critical buckling and postbuckling loads of cylindrical nanoshell. A new modified couple stress theory was employed for buckling analysis of anisotropic piezoelectric cylindrical shells subjected to axial compression and lateral pressure based on FSDT and considering von Karman geometric nonlinearity by Mehralian *et al*. (2016a). They concluded that the buckling loads are completely size-dependent and sensitive to small-scale parameter especially for large values of thickness and small values of length ratio. Zhang *et al*. (2015) studied free vibration analysis of a FG micro shell based on four unknown shear deformation theory and strain gradient theory. After evaluation of effective material properties using the Mori–Tanaka homogenization technique, the governing equations of motion have been derived based on Hamilton's principle. They concluded that the frequency and higher-order mode shapes are completely size-dependent when the thickness of micro-shell is reached to micro length scale parameter. Yeh (2016) studied vibration analysis of the sandwich cylindrical shells with MR elastomers based on Hamilton's principle and shear deformation theory. Lal *et al*. (2012) investigated stochastic

*Corresponding author, Professor,
E-mail: jsj@nut.edu.cn
[a] E-mail: dzx@nut.edu.cn



ISSN: 1738-1584 (Print), 1738-1991 (Online)

hygro-thermo-electro-mechanical post-buckling analysis of piezoelectric laminated cylindrical shell panel.

Ebrahimi *et al*. (2017) studied nonlocal strain gradient-based vibration analysis of embedded curved porous piezoelectric nano-beams in thermal environment. Nonlinear forced vibration analysis of a micro-shell reinforced by carbon nanotubes subjected to magnetic field and harmonic transverse loads was studied by Tohidi *et al*. (2018). The effect of agglomeration was included in the evaluation of material properties. The nonlinear vibration characteristics were evaluated in terms of important parameters of the problem such as magnetic field, CNTs volume percent and agglomeration effect. Size-dependent magneto-electro-elastic vibration analysis of cylindrical nanoshell was studied by Ke *et al*. (2014b) based on the nonlocal Love's shell theory. The differential quadrature method was used for the numerical solution of the problem in terms of nonlocal parameter, temperature rise, external electric and magnetic potential, radius-to-thickness ratio and length-to-radius ratio. Size dependent buckling analysis of functionally graded cylindrical micro shell was studied based on first order shear deformation theory and modified strain gradient theory by Gholami *et al*. (2014). The critical buckling loads have been evaluated in terms of small scale parameter and dimensionless geometric parameters. Shokrollahi (2018) employed differential quadrature method for static stress and deformation analysis of sandwich cylindrical shell. Some applications of size dependency in micro and nano scales were developed in various researches (Alam *et al*. 2020a, b, Zhang and Wang 2019, Zhao *et al*. 2020, Sun *et al*. 2020, Zhang *et al*. 2019, 2021, Zuo *et al*. 2017).

Free vibration analysis of a cylindrical nanoshell was studied by Rouhi *et al*. (2016) based on nonlinear shell model accounting surface elasticity theory. Nonlinearity was assumed based on von Kármán relations. Size-dependency was included in governing equations based on nonlocal elasticity theory. Modified couple stress theory was developed by Mehralian *et al*. (2016b) for size-dependent buckling analysis of shear deformable functionally graded cylindrical nanoshell based on first-order shear deformation theory. Functionality was assumed based on power-law distribution along the thickness direction. The critical pressure was calculated in terms of main parameters of the problem such as dimensionless geometrical parameters, material length scale parameter, length, thickness, applied voltage and in-homogeneous index. Salehipour *et al*. (2019) studied the static bending and free vibration characteristics of a functionally graded cylindrical micro and nano shells made of porous materials based on modified couple stress theory. The numerical results have been derived for simply and clamped boundary conditions. Ahmadi and Najafi (2016) studied static analysis of a rotating laminated composite cylindrical shell. Effect of rotating speed was studied on the stress distributions of composite shell. Arefi and Civalek (2020) developed Eringen nonlocal elasticity theory to static bending analysis of functionally graded cylindrical nanoshell in the framework of generalized Hooke's law and Energy method. Arefi *et al*. (2021) studied effect of graphene nanoplatelets as a novel reinforcement on the bending behaviors of composite cylindrical shell subjected to thermal and mechanical loads. Dehsaraji *et al*. (2020) studied effect of out of plane normal strains named as thickness stretching on the free vibration analysis of functionally graded cylindrical nanoshell using higher-order shear deformation theory.

Some researchers focused on the application of new materials in advanced manufacturing and energy resourcing (Abedini and Zhang 2021, Chao *et al*. 2020, Liu *et al*. 2020, Zuo *et al*. 2015, Li *et al*. 2020, Huang *et al*. 2021, Duan *et al*. 2021, Yin *et al*. 2021, Liu *et al*. 2021, Yang *et al*. 2017, Zhang *et al*. 2017, Wang *et al*. 2016). Lei and Tong (2019) studied free and forced vibration analysis of functionally graded cylindrical shell reinforced with graphene based on third-order shear deformation theory and Hamilton's principle using the Halpin-Tsai micromechanical model. Li *et al*. (2019) investigated free vibration analysis of uniform and stepped functionally graded cylindrical shells subjected to various boundary conditions based on first-order shear deformation theory. Haldar *et al*. (2019) employed a new nine isoparametric plate bending element for bending analysis of composite skew cylindrical shell based on first-order shear deformation theory. Four-unknown shear deformation theory was used for free vibration analysis of cylindrical micro-shell based on strain gradient elasticity theory by Zhang *et al*. (2015). Anitescu *et al*. (2019) developed a computational method for solving partial differential equations based on artificial neural networks and an adaptive collocation strategy. The Capability of the proposed method was developed in solving the important known problems such as Poisson and Helmholtz equations. Guo *et al*. (2019) solved bending analysis of a thin plate based on the deep collocation method. The proposed method was included a feedforward deep neural network through building a loss function for minimization of partial differential equations and boundary conditions at collocation. Rabczuk *et al*. (2019) proposed a new solution method of partial differential equations based on variational principle including a novel nonlocal operator. They summarized importance of the present method in solving the problems for eigenvalue analysis such as the waveguide problem through conversion into nonlocal integral form. Nguyen-Thanh *et al*. (2017) developed an isogeometric large deformation thin shell formulation for solving linear and nonlinear analyses of cylindrical and hemispherical shells, wind turbine rotor based on Nitsche's method. Areias *et al*. (2016) developed a new algorithm for elastic and elasto-plastic analysis of plates and shells based on phase-field model of crack regularization. Realistic behavior of fracture was modeled using two phase-fields related to upper and lower surfaces of shell. The formulation was developed based on finite strain model. Robustness and efficiency of the proposed method was confirmed using solution of the classic problems such as the Keesecker pressurized cylinder problem, the Hexcan problem, the Muscat-Fenech and Atkins plate. Areias and Rabczuk (2013) developed a new computational method based on finite element method for fracture analysis of plates and shells for brittle and ductile materials. Nanthakumar *et al*. (2016) proposed a new algorithm for solving the inverse

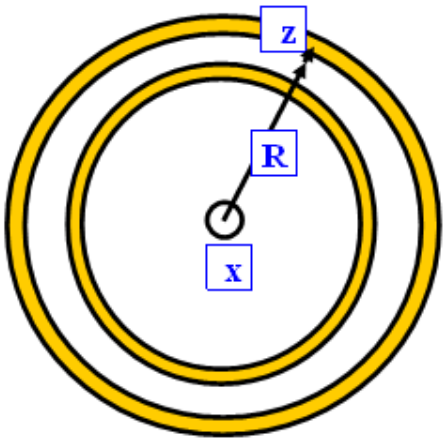


Fig. 1 The schematic of a three-layered micro shell

problem to detect inclusion interfaces in a piezoelectric structure. Each iteration of inverse problem was solved using extended finite element method. Vu-Bac *et al*. (2016) proposed a sensitivity analysis including a set of mathematical functions to study influence of uncertain input parameters on uncertain model outputs. The obtained results presented an important conclusion on the main input parameters of the problem.

Author presented comprehensive literature review on the related works including small scale analysis of structures, higher-order shear deformation theory and cylindrical micro- and nano-shells. It is confirmed based on author's knowledge, there is no published work on the higher-order electro-elastic analysis of functionally graded cylindrical micro-shell integrated with piezoelectric annular shells subjected to electrical and mechanical loads resting on Pasternak's foundation based on modified couple stress theory. This paper uses a higher-order model as kinematic relations and modified couple stress theory as a size-dependent theory for higher-order modeling of a micro cylindrical shell. For more accurate modeling the cylindrical micro shell specially shear strains, the third-order shear deformable model is used for variation of displacements along the axial and radial directions. The analytical solution is presented to investigate effect of significant parameters such as applied electric potential, micro length scale parameter, in-homogeneous index and two parameters of Pasternak's foundation.

## 2. Governing equations of three-layered cylindrical micro-shell

In this work, two-dimensional electro-elastic bending analysis of three-layered cylindrical micro-shell integrated with piezoelectric layers is presented based on third-order shear deformation theory and modified couple stress theory. The cylindrical shell is assumed subjected to electro-mechanical loads. The cylindrical shell is resting on Pasternak's foundation and two ends of it is constrained with simply-supported boundary conditions. Due to the symmetric distribution of material properties, boundary conditions and applied loadings, the transverse displacement is assumed zero. The displacement field is assumed along the axial and radial directions based on third-order shear deformation theory. The displacement field including axial and radial displacements is expressed as Arefi *et al*. (Arefi *et al*. 2018, Arefi 2013, Arefi and Rahimi 2011a, b, 2012a, b, c, Arefi and Zenkour 2018, 2019, Arefi *et al*. 2016)

$$\begin{aligned} u(x,z) &= u_0(x) + z\varphi_{x1}(x) + z^2\varphi_{x2}(x) + z^3\varphi_{x3}(x), \\ w(x,z) &= w_0(x) + z\varphi_{z1}(x) + z^2\varphi_{z2}(x) + z^3\varphi_{z3}(x) \end{aligned} \quad (1)$$

In which $u_0, u_0$ are axial and radial displacements of middle surface and $\varphi_{xi}, \varphi_{zi}$ are higher order rotation components.

The principle of virtual work $\delta U = \delta W$ is used to derive governing equations of a functionally graded micro-shell in which $U$ is the strain energy and $W$ is the work done by external forces. The variation of strain energy is defined as

$$\begin{aligned} \delta U_1 = \iiint_V (&\sigma_x \delta\varepsilon_x + \sigma_\theta \delta\varepsilon_\theta + \sigma_z \delta\varepsilon_z + \tau_{xz}\delta\gamma_{xz} \\ &- D_x \delta E_x - D_z \delta E_z)\, dV, \end{aligned} \quad (2)$$

where $\sigma_i, \varepsilon_i$ are stress and strain components and $D_i, E_i$ are electric displacement and electric field components. The stress components based on three-dimensional Hooke's law are expressed for functionally graded micro-core as (Khoshgoftar *et al*. 2013)

$$\begin{aligned} \sigma_x &= \lambda(z)\big[(1-\nu(z))\varepsilon_x + \nu(z)(\varepsilon_\theta + \varepsilon_z)\big], \\ \sigma_\theta &= \lambda(z)\big[(1-\nu(z))\varepsilon_\theta + \nu(z)(\varepsilon_x + \varepsilon_z)\big], \\ \sigma_z &= \lambda(z)\big[(1-\nu(z))\varepsilon_z + \nu(z)(\varepsilon_x + \varepsilon_\theta)\big], \\ \tau_{xz} &= \frac{E(z)}{2(1+\nu(z))}\gamma_{xz}, \end{aligned} \quad (3)$$

In which $\lambda(z) = E(z)/\big(1+\nu(z)\big)\big(1-2\nu(z)\big)$ and variable Young's modulus $E(z)$ and Poisson's ratio $\nu(z)$ are defined as $E(z) = (E_t - E_b)\left(\frac{z}{h}+\frac{1}{2}\right)^n + E_b$, $\nu(z) = (\nu_t - \nu_b)\left(\frac{z}{h}+\frac{1}{2}\right)^n + \nu_b$, where $E_t(\nu_t)$ and $E_b(\nu_b)$ are the values of the Young's modulus (Poisson's ratio) at the top and bottom surfaces, respectively, $n$ is the in-homogeneous index.

The electro-elastic constitutive relations for piezoelectric layers are expressed as

$$\begin{aligned} \sigma_x &= C_{xx}\varepsilon_x + C_{x\theta}\varepsilon_\theta + C_{xz}\varepsilon_z - e_{xzz}E_z, \\ \sigma_\theta &= C_{x\theta}\varepsilon_x + C_{\theta\theta}\varepsilon_\theta + C_{\theta z}\varepsilon_z - e_{\theta\theta z}E_z, \\ \sigma_z &= C_{xz}\varepsilon_x + C_{\theta z}\varepsilon_\theta + C_{zz}\varepsilon_z - e_{zzz}E_z, \\ \tau_{xz} &= C_{xzxz}\gamma_{xz} - e_{xzx}E_z, \\ D_x &= e_{xxz}\gamma_{xz} - \epsilon_{xx}E_x, \\ D_z &= e_{zxx}\varepsilon_x + e_{z\theta\theta}\varepsilon_\theta + e_{zzz}\varepsilon_z - \epsilon_{zz}E_z, \end{aligned} \quad (4)$$

In which $C_{ij}$, $e_{ijk}$, $\epsilon_{ij}$ are stiffness, piezoelectric and dielectric coefficients, respectively. Based on displacement field, the strain components are expressed as follows

$$\begin{aligned}
\varepsilon_x &= \frac{\mathrm{d}u}{\mathrm{d}x} = \frac{\mathrm{d}u_0}{\mathrm{d}x} + z\frac{\mathrm{d}\varphi_{x1}}{\mathrm{d}x} + z^2\frac{\mathrm{d}\varphi_{x2}}{\mathrm{d}x} + z^3\frac{\mathrm{d}\varphi_{x3}}{\mathrm{d}x},\\
\varepsilon_z &= \frac{\mathrm{d}w}{\mathrm{d}z} = \varphi_{z1} + 2z\varphi_{z2} + 3z^2\varphi_{z3},\\
\varepsilon_\theta &= \frac{1}{R+z}w_0 + \frac{z}{R+z}\varphi_{z1} + \frac{z^2}{R+z}\varphi_{z2} + \frac{z^3}{R+z}\varphi_{z3},\\
\gamma_{xz} &= \frac{\mathrm{d}u}{\mathrm{d}z} + \frac{\mathrm{d}w}{\mathrm{d}x} = \varphi_{x1} + 2z\varphi_{x2} + 3z^2\varphi_{x3} + \frac{dw_0}{dx} + z\frac{\mathrm{d}\varphi_{z1}}{\mathrm{d}x} + z^2\frac{\mathrm{d}\varphi_{z2}}{\mathrm{d}x} + z^3\frac{\mathrm{d}\varphi_{z3}}{\mathrm{d}x},
\end{aligned} \tag{5}$$

Electric field components are derived using electric potential function. The electric potential is defined as

$$\Phi(x,z) = \frac{2\check{z}}{h}\Phi_0 - \Phi(x)cos\frac{\pi\check{z}}{h} \tag{6}$$

Electric field components are defined using minus divergence of electric potential $E_i = -\Phi_{,i}$ as follows

$$E_x = \frac{\partial\Phi}{\partial x}cos\frac{\pi\check{z}}{h}, \qquad E_z = -\frac{2\Phi_0}{h} - \frac{\pi}{h}\Phi sin\frac{\pi\check{z}}{h} \tag{7}$$

Based on definition of electric field and strain field components, the constitutive electro-elastic relations are:

To account size-dependency in micro-scale, MCST is used. Based on this theory, strain energy is obtained as

$$\delta U_2 = \int_V m_{ij}\delta\chi_{ij}dx. \tag{8}$$

In which $m_{ij}$ and $\chi_{ij}$ are defined as follows

$$m_{ij} = \frac{E}{1+\nu}l^2\chi_{ij}. \tag{9}$$

$\chi_{ij}$ are defined as

$$\chi = \frac{1}{2}\left(\overrightarrow{\nabla\theta} + \left(\overrightarrow{\nabla\theta}\right)^T\right). \tag{10}$$

where $\theta_i$ are defined as

$$\theta = \frac{1}{2}curl\vec{\mathrm{u}}. \tag{11}$$

The components of rotation vector $\vec{\theta}$ are defined as follows

$$\begin{aligned}
curl\vec{\mathrm{u}} = {} & (g_{22}g_{33})^{-1/2}\left(\frac{\partial\left(\sqrt{g_{33}}u_3\right)}{\partial x_2} - \frac{\partial\left(\sqrt{g_{22}}u_2\right)}{\partial x_3}\right)\overrightarrow{e_1} + (g_{11}g_{33})^{-1/2}\left(\frac{\partial\left(\sqrt{g_{11}}u_1\right)}{\partial x_3} - \frac{\partial\left(\sqrt{g_{33}}u_3\right)}{\partial x_1}\right)\overrightarrow{e_2}\\
& + (g_{11}g_{22})^{-1/2}\left(\frac{\partial\left(\sqrt{g_{22}}u_2\right)}{\partial x_1} - \frac{\partial\left(\sqrt{g_{11}}u_1\right)}{\partial x_2}\right)\overrightarrow{e_3},
\end{aligned} \tag{12}$$

In which $g_{11}$, $g_{22}$, $g_{33}$ are defined as follows

$$g_{22} = 1, \qquad g_{22} = (R+z)^2, \qquad g_{33} = 1, \tag{13}$$

Based on TSDT, we will have

$$\begin{aligned}
\vec{\theta} = \frac{1}{2}\Big(\varphi_{x1} - \frac{\partial w_0}{\partial x} + z\left(2\varphi_{x2} - \frac{\partial\varphi_{z1}}{\partial x}\right)\\
+ z^2\left(3\varphi_{x3} - \frac{\partial\varphi_{z2}}{\partial x}\right) - z^3\frac{\partial\varphi_{z3}}{\partial x}\Big)\overrightarrow{e_2}.
\end{aligned} \tag{14}$$

After derivation of the components of the symmetric curvature tensor, the deviatoric part of the symmetric couple stress tensor can be derived from.

$$m_{z\theta} = \frac{E}{1+\nu} l^2 \frac{1}{4}\left(2\varphi_{x2} - \frac{\partial \varphi_{z1}}{\partial x} + 2z\left(3\varphi_{x3} - \frac{\partial \varphi_{z2}}{\partial x}\right) - 3z^2 \frac{\partial \varphi_{z3}}{\partial x} - \frac{\varphi_{x1}}{R+z} + \frac{1}{R+z}\frac{\partial w_0}{\partial x} - \frac{z}{R+z}\left(2\varphi_{x2} - \frac{\partial \varphi_{z1}}{\partial x}\right) - \frac{z^2}{R+z}\left(3\varphi_{x3} - \frac{\partial \varphi_{z2}}{\partial x}\right) + \frac{z^3}{R+z}\frac{\partial \varphi_{z3}}{\partial x}\right). \tag{15}$$

The strain energy associated with modified couple stress theory is derived as

$$\delta U_2 = 2\pi \int_V \frac{1}{4} \begin{pmatrix} P^1_{z\theta}\left(2\delta\varphi_{x2} - \frac{\partial \delta\varphi_{z1}}{\partial x}\right) \\ +2P^2_{z\theta}\left(3\delta\varphi_{x3} - \frac{\partial \delta\varphi_{z2}}{\partial x}\right) \\ -3P^3_{z\theta}\frac{\partial \delta\varphi_{z3}}{\partial x} + M^1_{z\theta}\left(\frac{\partial \delta w_0}{\partial x} - \delta\varphi_{x1}\right) \\ -M^2_{z\theta}\left(2\delta\varphi_{x2} - \frac{\partial \delta\varphi_{z1}}{\partial x}\right) \\ -M^3_{z\theta}\left(3\delta\varphi_{x3} - \frac{\partial \delta\varphi_{z2}}{\partial x}\right) + M^4_{z\theta}\frac{\partial \delta\varphi_{z3}}{\partial x} \end{pmatrix} dx. \tag{16}$$

In which the resultant components are defined as

$$\begin{aligned} M^i_{z\theta} &= \frac{1}{4}\int_{-\frac{h}{2}}^{\frac{h}{2}} m_{z\theta} z^{(i-1)} dz\,, \qquad i = 1,2,3,4 \\ P^i_{z\theta} &= \frac{1}{4}\int_{-\frac{h}{2}}^{\frac{h}{2}} m_{z\theta}(R+z) z^{(i-1)} dz \qquad i = 1,2,3. \end{aligned} \tag{17}$$

Integration by part on Eq. (18) leads to

$$\delta U_2 = 2\pi \int_V \begin{pmatrix} -M^1_{z\theta}\delta\varphi_{x1} + (2P^1_{z\theta} - 2M^2_{z\theta})\delta\varphi_{x2} + (6P^2_{z\theta} - 3M^3_{z\theta})\delta\varphi_{x3} - \frac{\partial M^1_{z\theta}}{\partial x}\delta w_0 \\ +\left(\frac{\partial P^1_{z\theta}}{\partial x} - \frac{\partial M^2_{z\theta}}{\partial x}\right)\delta\varphi_{z1} + \left(2\frac{\partial P^2_{z\theta}}{\partial x} - \frac{\partial M^3_{z\theta}}{\partial x}\right)\delta\varphi_{z2} + \left(3\frac{\partial P^3_{z\theta}}{\partial x} - \frac{\partial M^4_{z\theta}}{\partial x}\right)\delta\varphi_{z3} \end{pmatrix} dx. \tag{18}$$

The strain energy associated with Cauchy stress components (Eq. (2)) are defined as

$$\begin{aligned} \delta U_1 = 2\pi \iiint_V \Big( &\left[N_x \frac{\mathrm{d}\delta u_0}{\mathrm{d}x} + M_x \frac{\mathrm{d}\delta\varphi_{x1}}{\mathrm{d}x} + S_x \frac{\mathrm{d}\delta\varphi_{x2}}{\mathrm{d}x} + P_x \frac{\mathrm{d}\delta\varphi_{x3}}{\mathrm{d}x}\right] + [N_\theta \delta w_0 + M_\theta \delta\varphi_{z1} + S_\theta \delta\varphi_{z2} + P_\theta \delta\varphi_{z3}] \\ &+[N_z \delta\varphi_{z1} + 2M_z \delta\varphi_{z2} + 3S_z \delta\varphi_{z3}] + \left[N_{xz}\delta\varphi_{x1} + 2M_{xz}\delta\varphi_{x2} + 3S_{xz}\delta\varphi_{x3} + N_{xz}\frac{d\delta w_0}{dx}\right. \\ &\left. +M_{xz}\frac{\mathrm{d}\delta\varphi_{z1}}{\mathrm{d}x} + S_{xz}\frac{\mathrm{d}\delta\varphi_{z2}}{\mathrm{d}x} + P_{xz}\frac{\mathrm{d}\delta\varphi_{z3}}{\mathrm{d}x}\right] - \overline{D_x}\frac{\partial\delta\Phi}{\partial x} + \overline{D_z}\delta\Phi\Big)\,\mathrm{dx}. \end{aligned} \tag{19}$$

where the resultants of forces and moments.

Integration by part on Eq. (21) leads to following relation

$$\begin{aligned} \delta U = \int_0^l \Bigg[ &-\frac{\mathrm{d}N_x}{\mathrm{d}x}\delta u_0 + \left[N_{xz} - \frac{\mathrm{d}M_x}{\mathrm{d}x}\right]\delta\varphi_{x1} + \left[2M_{xz} - \frac{\mathrm{d}S_x}{\mathrm{d}x}\right]\delta\varphi_{x2} + \left[3S_{xz} - \frac{\mathrm{d}P_x}{\mathrm{d}x}\right]\delta\varphi_{x3} + \left[N_\theta - \frac{dN_{xz}}{dx}\right]\delta w_0 \\ &+ \left[M_\theta + N_z - \frac{\mathrm{d}M_{xz}}{\mathrm{d}x}\right]\delta\varphi_{z1} + \left[S_\theta + 2M_z - \frac{\mathrm{d}S_{xz}}{\mathrm{d}x}\right]\delta\varphi_{z2} + \left[P_\theta + 3S_z - \frac{\mathrm{d}P_{xz}}{\mathrm{d}x}\right]\delta\varphi_{z3} \\ &+ \left[\frac{\partial\overline{D_x}}{\partial x} + \overline{D_z}\right]\delta\Phi\Bigg] dx. \end{aligned} \tag{20}$$

The virtual work done by external forces is defined as follows

$$\begin{aligned}\delta W &= \int_0^l \left[P_i \delta u_z|_{z=-\frac{h}{2}} - F_f \delta u_z|_{z=\frac{h}{2}}\right] \mathrm{d}x \\ &= -\int_0^l \left\{P_i[w_0 + z\varphi_{z1} + z^2\varphi_{z2} + z^3\varphi_{z3}]|_{z=-\frac{h}{2}} - F_f[w_0 + z\varphi_{z1} + z^2\varphi_{z2} + z^3\varphi_{z3}]\big|_{z=+\frac{h}{2}}\right\} \mathrm{d}x,\end{aligned} \tag{22}$$

where $F_f$ is expressed as $F_f = K_1 u_z - K_2 \nabla^2 u_z$ . Substitution of radial displacement into reaction of Pasternak foundation leads to following relation

$$F_f = K_1\left(w_0 + \frac{h}{2}\varphi_{z1} + \left(\frac{h}{2}\right)^2 \varphi_{z2} + \left(\frac{h}{2}\right)^3 \varphi_{z3}\right) - K_2\left(\frac{\mathrm{d}^2 w_0}{\mathrm{d}x^2} + + \frac{h}{2}\frac{\mathrm{d}^2\varphi_{z1}}{\mathrm{d}x^2} + \left(\frac{h}{2}\right)^2 \frac{\mathrm{d}^2\varphi_{z2}}{\mathrm{d}x^2} + \left(\frac{h}{2}\right)^3 \frac{\mathrm{d}^2\varphi_{z3}}{\mathrm{d}x^2}\right), \tag{23}$$

By substitution of strain energy and external work into principle of virtual work, the final governing equations are derived as

$$\begin{aligned}
&\delta u_0 : -\frac{\mathrm{d}N_x}{\mathrm{d}x} = 0, \\
&\delta\varphi_{x1} : N_{xz} - \frac{\mathrm{d}M_x}{\mathrm{d}x} - M_{z\theta}^1 = 0, \\
&\delta\varphi_{x2} : 2M_{xz} - \frac{\mathrm{d}S_x}{\mathrm{d}x} + 2P_{z\theta}^1 - 2M_{z\theta}^2 = 0, \\
&\delta\varphi_{x3} : 3S_{xz} - \frac{\mathrm{d}P_x}{\mathrm{d}x} + 6P_{z\theta}^2 - 3M_{z\theta}^3 = 0, \\
&\delta w_0 : N_\theta - \frac{dN_{xz}}{dx} - \frac{\partial M_{z\theta}^1}{\partial x} = P_i\left(R - \frac{h}{2}\right) - F_f\left(R + \frac{h}{2}\right) \\
&\delta\varphi_{z1} : M_\theta + N_z - \frac{\mathrm{d}M_{xz}}{\mathrm{d}x} + \frac{\partial P_{z\theta}^1}{\partial x} - \frac{\partial M_{z\theta}^2}{\partial x} = -\frac{h}{2}\left[P_i\left(R - \frac{h}{2}\right) + F_f\left(R + \frac{h}{2}\right)\right] \\
&\delta\varphi_{z2} : S_\theta + 2M_z - \frac{\mathrm{d}S_{xz}}{\mathrm{d}x} + 2\frac{\partial P_{z\theta}^2}{\partial x} - \frac{\partial M_{z\theta}^3}{\partial x} = \left(\frac{h}{2}\right)^2\left[P_i\left(R - \frac{h}{2}\right) - F_f\left(R + \frac{h}{2}\right)\right] \\
&\delta\varphi_{z3} : P_\theta + 3S_z - \frac{\mathrm{d}P_{xz}}{\mathrm{d}x} + 3\frac{\partial P_{z\theta}^3}{\partial x} - \frac{\partial M_{z\theta}^4}{\partial x} = -\left(\frac{h}{2}\right)^3\left[P_i\left(R - \frac{h}{2}\right) + F_f\left(R + \frac{h}{2}\right)\right] \\
&\delta\Phi : \frac{\partial\overline{D_x}}{\partial x} + \overline{D_z} = 0
\end{aligned} \tag{24}$$

where the size-dependent resultant forces and moments expressed by the displacements have the following forms

$$\begin{Bmatrix} N_x \\ M_x \\ S_x \\ P_x \\ N_z \\ M_z \\ S_z \\ N_\theta \\ M_\theta \\ S_\theta \\ P_\theta \\ \overline{D_z} \end{Bmatrix} = \begin{bmatrix} A_1 & A_2 & & A_3 & A_4 & A_5 & A_6 + A_9 & A_7 + A_{10} & A_8 + A_{11} & A_{150} \\ A_{30} & A_{31} & & A_{32} & A_{33} & A_{34} & A_{35} + A_{38} & A_{36} + A_{39} & A_{37} + A_{40} & A_{152} \\ A_{59} & A_{60} & A_{61} & A_{62} & A_{63} & A_{64} + A_{67} & A_{65} + A_{68} & A_{66} + A_{69} & A_{154} & \\ A_{88} & A_{89} & A_{90} & A_{91} & A_{92} & A_{93} + A_{96} & A_{94} + A_{97} & A_{95} + A_{98}A_{156} & & \\ A_{15} & A_{16} & A_{17} & A_{18} & A_{19} & A_{12} + A_{20} & A_{13} + A_{21} & A_{14} + A_{22}A_{151} & & \\ A_{44} & A_{45} & A_{46} & A_{47} & A_{48} & A_{41} + A_{49} & A_{42} + A_{50} & A_{43} + A_{51}A_{153} & & \\ A_{73} & A_{74} & A_{75} & A_{76} & A_{77} & A_{70} + A_{78} & A_{71} + A_{79} & A_{72} + A_{80}A_{155} & & \\ A_{110} & A_{111} & A_{112} & A_{113} & A_{106} & A_{107} + A_{114} & A_{108} + A_{115} & A_{109} + A_{116}A_{161} & & \\ A_{212} & A_{122} & A_{123} & A_{124} & A_{117} & A_{118} + A_{125} & A_{119} + A_{126} & A_{120} + A_{127}A_{162} & & \\ A_{132} & A_{133} & A_{134} & A_{135} & A_{128} & A_{129} + A_{136} & A_{130} + A_{137} & A_{131} + A_{138}A_{163} & & \\ A_{143} & A_{144} & A_{145} & A_{146} & A_{139} & A_{140} + A_{147} & A_{141} + A_{148} & A_{142} + A_{149}A_{164} & & \\ A_{170} & A_{171} & A_{172} & A_{173} & A_{174} & A_{175} + A_{178} & A_{176} + 2A_{179} & A_{177} + 3A_{180} & -A_{181} & \end{bmatrix} \begin{Bmatrix} \frac{\mathrm{d}u_0}{\mathrm{d}x} \\ \frac{\mathrm{d}u_{x1}}{\mathrm{d}x} \\ \frac{\mathrm{d}u_{x2}}{\mathrm{d}x} \\ \frac{\mathrm{d}u_{x3}}{\mathrm{d}x} \\ w_0 \\ w_{z1} \\ w_{z2} \\ w_{z3} \\ \Phi \end{Bmatrix} + \begin{Bmatrix} N_x^{\Phi_0} \\ M_x^{\Phi_0} \\ S_x^{\Phi_0} \\ P_x^{\Phi_0} \\ N_z^{\Phi_0} \\ M_z^{\Phi_0} \\ S_z^{\Phi_0} \\ N_\theta^{\Phi_0} \\ M_\theta^{\Phi_0} \\ S_\theta^{\Phi_0} \\ P_\theta^{\Phi_0} \\ -D_z^{\Phi_0} \end{Bmatrix}. \tag{25}$$

And

$$\begin{Bmatrix} N_{xz} \\ M_{xz} \\ S_{xz} \\ P_{xz} \\ \overline{D_x} \end{Bmatrix} = \begin{bmatrix} A_{23} & A_{24} & A_{25} & A_{26} & A_{27} & A_{28} & A_{29} & A_{157} \\ A_{52} & A_{53} & A_{54} & A_{55} & A_{56} & A_{57} & A_{58} & A_{158} \\ A_{81} & A_{82} & A_{83} & A_{84} & A_{85} & A_{86} & A_{87} & A_{159} \\ A_{99} & A_{100} & A_{101} & A_{102} & A_{103} & A_{104} & A_{105} & A_{160} \\ A_{165} & 2A_{166} & 3A_{167} & A_{165} & A_{166} & A_{167} & A_{168} & -A_{169} \end{bmatrix} \begin{Bmatrix} u_{x1} \\ u_{x2} \\ u_{x3} \\ \dfrac{dw_0}{dx} \\ \dfrac{\mathrm{d}w_{z1}}{\mathrm{d}x} \\ \dfrac{\mathrm{d}w_{z2}}{\mathrm{d}x} \\ \dfrac{\mathrm{d}w_{z3}}{\mathrm{d}x} \\ -\dfrac{\partial \Phi}{\partial x} \end{Bmatrix}. \tag{26}$$

Substitution of the resultant forces and moments into governing equations gives

$$\begin{aligned}
\delta u_0: \quad & -A_1\frac{\mathrm{d}^2u_0}{\mathrm{d}x^2} - A_2\frac{\mathrm{d}^2\varphi_{x1}}{\mathrm{d}x^2} - A_3\frac{\mathrm{d}^2\varphi_{x2}}{\mathrm{d}x^2} - A_4\frac{\mathrm{d}^2\varphi_{x3}}{\mathrm{d}x^2} - A_5\frac{\mathrm{d}w_0}{\mathrm{d}x} - (A_6+A_9)\frac{\mathrm{d}\varphi_{z1}}{\mathrm{d}x} \\
& -(A_7+A_{10})\frac{\mathrm{d}\varphi_{z2}}{\mathrm{d}x} - (A_8+A_{11})\frac{\mathrm{d}\varphi_{z3}}{\mathrm{d}x} - A_{150}\frac{\mathrm{d}\Phi}{dx} = \frac{\mathrm{d}N_x^{\Phi_0}}{dx} \\
\delta\varphi_{x1}: \quad & -A_{30}\frac{\mathrm{d}^2u_0}{\mathrm{d}x^2} - A_{31}\frac{\mathrm{d}^2\varphi_{x1}}{\mathrm{d}x^2} + (A_{23}+C_{153})\varphi_{x1} - A_{32}\frac{\mathrm{d}^2\varphi_{x2}}{\mathrm{d}x^2} + (A_{24}+2C_{154}-2C_{150})\varphi_{x2} - A_{33}\frac{\mathrm{d}^2\varphi_{x3}}{\mathrm{d}x^2} \\
& +(A_{25}+3C_{155}-6C_{151})\varphi_{x3} + (A_{26}-A_{34}-C_{153})\frac{\mathrm{d}w_0}{\mathrm{d}x} + (A_{27}-A_{35}-A_{38}-C_{154}+C_{150})\frac{\mathrm{d}\varphi_{z1}}{\mathrm{d}x} \\
& +(A_{28}-A_{36}-A_{39}+2C_{151}-C_{155})\frac{\mathrm{d}\varphi_{z2}}{\mathrm{d}x} + (A_{29}-A_{37}-A_{40}-C_{156}+3C_{152})\frac{\mathrm{d}\varphi_{z3}}{\mathrm{d}x} \\
& -(A_{157}+A_{152})\frac{\partial\Phi}{\partial x} = \frac{\partial M_x^{\Phi_0}}{\partial x}, \\
\delta\varphi_{x2}: \quad & -A_{59}\frac{\mathrm{d}^2u_0}{\mathrm{d}x^2} - A_{60}\frac{\mathrm{d}^2\varphi_{x1}}{\mathrm{d}x^2} + (2A_{52}-2C_{150}+2C_{154})\varphi_{x1} - A_{61}\frac{\mathrm{d}^2\varphi_{x2}}{\mathrm{d}x^2} \\
& +(2A_{53}+4C_{163}-4C_{151}-4C_{151}+4C_{155})\varphi_{x2} - A_{62}\frac{\mathrm{d}^2\varphi_{x3}}{\mathrm{d}x^2} \\
& +(2A_{54}+12C_{164}-6C_{152}-12C_{152}+6C_{156})\varphi_{x3} + (2A_{55}-A_{63}+2C_{150}-2C_{154})\frac{\mathrm{d}w_0}{\mathrm{d}x} \\
& +(2A_{56}-A_{67}-A_{64}-2C_{163}+2C_{151}+2C_{151}-2C_{155})\frac{\mathrm{d}\varphi_{z1}}{\mathrm{d}x} \\
& +(2A_{57}-A_{65}-A_{68}+2A_{58}-A_{66}-A_{69}-4C_{164}+2C_{152}+4C_{152}-2C_{156})\frac{\mathrm{d}\varphi_{z2}}{\mathrm{d}x} \\
& +(2C_{157}-6C_{165}+6C_{157}-2C_{158})\frac{\partial\varphi_{z3}}{\partial x} - (2A_{158}+A_{154})\frac{\partial\Phi}{\partial x} = \frac{\partial S_x^{\Phi_0}}{\partial x}, \\
\delta\varphi_{x3}: \quad & -A_{88}\frac{\mathrm{d}^2u_0}{\mathrm{d}x^2} - A_{89}\frac{\mathrm{d}^2\varphi_{x1}}{\mathrm{d}x^2} + (3A_{81}-6C_{151}+3C_{155})\varphi_{x1} - A_{90}\frac{\mathrm{d}^2\varphi_{x2}}{\mathrm{d}x^2} \\
& +(3A_{82}+12C_{164}-6C_{152}+6C_{156}-12C_{152})\varphi_{x2} - A_{91}\frac{\mathrm{d}^2\varphi_{x3}}{\mathrm{d}x^2} \\
& +(3A_{83}+36C_{165}-18C_{157}-18C_{157}+9C_{158})\varphi_{x3} + (3A_{84}-A_{92}-3C_{155}+6C_{151})\frac{\mathrm{d}w_0}{\mathrm{d}x} \\
& +(3A_{85}-A_{96}-A_{93}-6C_{164}+6C_{152}+3C_{152}-3C_{156})\frac{\mathrm{d}\varphi_{z1}}{\mathrm{d}x} \\
& +(3A_{86}-A_{94}-A_{97}+6C_{157}-12C_{165}+6C_{157})\frac{\mathrm{d}\varphi_{z2}}{\mathrm{d}x} \\
& +(3A_{87}-A_{95}-A_{98}+6C_{159}-18C_{166}+9C_{159}-3C_{158}-3C_{160})\frac{\mathrm{d}\varphi_{z3}}{\mathrm{d}x} - (3A_{159}+A_{156})\frac{\partial\Phi}{\partial x} = \frac{\partial P_x^{\Phi_0}}{\partial x}, \\
\delta w_0: \quad & A_{110}\frac{\mathrm{d}u_0}{\mathrm{d}x} + (A_{111}-A_{23}+C_{153})\frac{\mathrm{d}\varphi_{x1}}{\mathrm{d}x} + (A_{112}-A_{24}+2C_{154}-2C_{150})\frac{\mathrm{d}\varphi_{x2}}{\mathrm{d}x} \\
& +(A_{113}-A_{25}-6C_{151}+3C_{155})\frac{\mathrm{d}\varphi_{x3}}{\mathrm{d}x} - (A_{26}+C_{153})\frac{d^2w_0}{dx^2} + A_{106}w_0 + (C_{150}-A_{27}-C_{154})\frac{\mathrm{d}^2\varphi_{z1}}{\mathrm{d}x^2} \\
& +(A_{107}+A_{114})\varphi_{z1} + (2C_{151}-A_{28}-C_{155})\frac{\mathrm{d}^2\varphi_{z2}}{\mathrm{d}x^2} + (A_{108}+A_{115})\varphi_{z2} + (3C_{152}-C_{156}-A_{29})\frac{\mathrm{d}^2\varphi_{z3}}{\mathrm{d}x^2}
\end{aligned} \tag{27}$$

$$+(A_{109}+A_{116})\varphi_{z3}+A_{161}\Phi+A_{157}\frac{\mathrm{d}^2\Phi}{\mathrm{d}x^2}=-N_\theta^{\Phi_0}+P_i\left(R-\frac{h}{2}\right)-\left[K_1\left(w_0+\frac{h}{2}\varphi_{z1}+\left(\frac{h}{2}\right)^2\varphi_{z2}+\left(\frac{h}{2}\right)^3\varphi_{z3}\right)\right.$$
$$\left.-K_2\left(\frac{\mathrm{d}^2w_0}{\mathrm{d}x^2}++\frac{h}{2}\frac{\mathrm{d}^2\varphi_{z1}}{\mathrm{d}x^2}+\left(\frac{h}{2}\right)^2\frac{\mathrm{d}^2\varphi_{z2}}{\mathrm{d}x^2}+\left(\frac{h}{2}\right)^3\frac{\mathrm{d}^2\varphi_{z3}}{\mathrm{d}x^2}\right)\right]\left(R+\frac{h}{2}\right)\Bigg]$$

$\delta\varphi_{z1}$:
$$(A_{15}+A_{121})\frac{\mathrm{d}u_0}{\mathrm{d}x}+(A_{16}+A_{122}-A_{52}-C_{150}+C_{154})\frac{\mathrm{d}\varphi_{x1}}{\mathrm{d}x}$$
$$+(A_{123}+A_{17}-A_{53}+2C_{163}-2C_{151}-2C_{151}+2C_{155})\frac{\mathrm{d}\varphi_{x2}}{\mathrm{d}x}$$
$$+(A_{124}-A_{54}+A_{18}-3C_{152}+3C_{156}+6C_{164}-6C_{152})\frac{\mathrm{d}\varphi_{x3}}{\mathrm{d}x}+(A_{117}+A_{19})w_0+(C_{150}-C_{154}-A_{55})\frac{d^2w_0}{dx^2}$$
$$+(A_{12}+A_{20}+A_{118}+A_{125})\varphi_{z1}+C_{151}\frac{\mathrm{d}^2\varphi_{z1}}{\mathrm{d}x^2}-C_{155}\frac{\mathrm{d}^2\varphi_{z1}}{\mathrm{d}x^2}-A_{56}\frac{\mathrm{d}^2\varphi_{z1}}{\mathrm{d}x^2}-C_{163}\frac{\mathrm{d}^2\varphi_{z1}}{\mathrm{d}x^2}+C_{151}\frac{\mathrm{d}^2\varphi_{z1}}{\mathrm{d}x^2}$$
$$+(A_{13}+A_{21}+A_{119}+A_{126})\varphi_{z2}+(C_{152}+2C_{152}-A_{57}-2C_{164}-C_{156})\frac{\mathrm{d}^2\varphi_{z2}}{\mathrm{d}x^2}$$
$$+(A_{14}+A_{120}+A_{22}+A_{127})\varphi_{z3}+(C_{157}+3C_{157}-A_{58}-3C_{165}-C_{158})\frac{\mathrm{d}^2\varphi_{z3}}{\mathrm{d}x^2}+(A_{151}+A_{162})\Phi$$
$$+A_{158}\frac{\mathrm{d}^2\Phi}{\mathrm{d}x^2}=-N_z^{\Phi_0}-M_\theta^{\Phi_0}-\frac{h}{2}\left[P_i\left(R-\frac{h}{2}\right)+\left[K_1\left(w_0+\frac{h}{2}\varphi_{z1}+\left(\frac{h}{2}\right)^2\varphi_{z2}+\left(\frac{h}{2}\right)^3\varphi_{z3}\right)\right.\right.$$
$$\left.\left.-K_2\left(\frac{\mathrm{d}^2w_0}{\mathrm{d}x^2}++\frac{h}{2}\frac{\mathrm{d}^2\varphi_{z1}}{\mathrm{d}x^2}+\left(\frac{h}{2}\right)^2\frac{\mathrm{d}^2\varphi_{z2}}{\mathrm{d}x^2}+\left(\frac{h}{2}\right)^3\frac{\mathrm{d}^2\varphi_{z3}}{\mathrm{d}x^2}\right)\right]\left(R+\frac{h}{2}\right)\right]$$

$\delta\varphi_{z2}$:
$$(2A_{44}+A_{132})\frac{\mathrm{d}u_0}{\mathrm{d}x}+(A_{133}+2A_{45}-A_{81}-2C_{151}+C_{155})\frac{\mathrm{d}\varphi_{x1}}{\mathrm{d}x}$$
$$+(A_{134}+2A_{46}-A_{82}+4C_{164}-2C_{152}+2C_{156}-4C_{152})\frac{\mathrm{d}\varphi_{x2}}{\mathrm{d}x}$$
$$+(A_{135}+2A_{47}-A_{83}+12C_{165}-6C_{157}-6C_{157}+3C_{158})\frac{\mathrm{d}\varphi_{x3}}{\mathrm{d}x}+(2C_{151}-A_{84}-C_{155})\frac{d^2w_0}{dx^2}$$
$$+(2A_{48}+A_{128})w_0+(C_{152}-A_{85}-2C_{164}+2C_{152}-C_{156})\frac{\mathrm{d}^2\varphi_{z1}}{\mathrm{d}x^2}+(2A_{41}+2A_{49}+A_{129}+A_{136})\varphi_{z1} \tag{27}$$
$$+(2C_{157}-A_{86}-4C_{165}+2C_{157}-C_{158})\frac{\mathrm{d}^2\varphi_{z2}}{\mathrm{d}x^2}+(A_{130}+2A_{42}+2A_{50}+A_{137})\varphi_{z2}$$
$$+(C_{159}+3C_{159}-C_{160}-6C_{166})\frac{\mathrm{d}^2\varphi_{z3}}{\mathrm{d}x^2}-A_{87}\frac{\mathrm{d}^2\varphi_{z3}}{\mathrm{d}x^2}+(A_{131}+A_{138}+2A_{43}+2A_{51})\varphi_{z3}$$
$$+(A_{163}+2A_{153})\Phi+A_{159}\frac{\mathrm{d}^2\Phi}{\mathrm{d}x^2}=-S_\theta^{\Phi_0}-2M_z^{\Phi_0}$$
$$+\left(\frac{h}{2}\right)^2\left[P_i\left(R-\frac{h}{2}\right)-\left[K_1\left(w_0+\frac{h}{2}\varphi_{z1}+\left(\frac{h}{2}\right)^2\varphi_{z2}+\left(\frac{h}{2}\right)^3\varphi_{z3}\right)\right.\right.$$
$$\left.\left.-K_2\left(\frac{\mathrm{d}^2w_0}{\mathrm{d}x^2}+\frac{h}{2}\frac{\mathrm{d}^2\varphi_{z1}}{\mathrm{d}x^2}+\left(\frac{h}{2}\right)^2\frac{\mathrm{d}^2\varphi_{z2}}{\mathrm{d}x^2}+\left(\frac{h}{2}\right)^3\frac{\mathrm{d}^2\varphi_{z3}}{\mathrm{d}x^2}\right)\right]\left(R+\frac{h}{2}\right)\right.$$

$\delta\varphi_{z3}$:
$$(3A_{73}+A_{143})\frac{\mathrm{d}u_0}{\mathrm{d}x}+(3A_{74}+A_{144}-A_{99}-3C_{152}+C_{156})\frac{\mathrm{d}\varphi_{x1}}{\mathrm{d}x}$$
$$+(3A_{75}+A_{145}-A_{100}+6C_{165}-2C_{157}-6C_{157}+2C_{158})\frac{\mathrm{d}\varphi_{x2}}{\mathrm{d}x}$$
$$+(A_{146}-A_{101}+3A_{76}+18C_{166}-6C_{159}-9C_{159}+3C_{160})\frac{\mathrm{d}\varphi_{x3}}{\mathrm{d}x}+(3C_{152}-C_{156}-A_{102})\frac{d^2w_0}{dx^2}$$
$$+(3A_{77}+A_{139})w_0+(3C_{157}-3C_{165}-C_{158}+C_{157}-A_{103})\frac{\mathrm{d}^2\varphi_{z1}}{\mathrm{d}x^2}+(A_{140}\varphi_{z1}+3A_{78}+3A_{70}+A_{147})\varphi_{z1}$$
$$+(2C_{159}-A_{104}-6C_{166}+3C_{159}-C_{160})\frac{\mathrm{d}^2\varphi_{z2}}{\mathrm{d}x^2}+(A_{141}+A_{148}+3A_{71}+3A_{79})\varphi_{z2}$$
$$+(3C_{161}+3C_{161}-C_{162}-9C_{167}-A_{105})\frac{\mathrm{d}^2\varphi_{z3}}{\mathrm{d}x^2}+(A_{149}+3A_{80}+A_{142}+3A_{72})\varphi_{z3}+(A_{164}+3A_{155})\Phi$$
$$+A_{160}\frac{\mathrm{d}^2\Phi}{\mathrm{d}x^2}=-P_\theta^{\Phi_0}-3S_z^{\Phi_0}-\left(\frac{h}{2}\right)^3\left[P_i\left(R-\frac{h}{2}\right)+\left[K_1\left(w_0+\frac{h}{2}\varphi_{z1}+\left(\frac{h}{2}\right)^2\varphi_{z2}+\left(\frac{h}{2}\right)^3\varphi_{z3}\right)\right.\right.$$
$$\left.\left.-K_2\left(\frac{\mathrm{d}^2w_0}{\mathrm{d}x^2}+\frac{h}{2}\frac{\mathrm{d}^2\varphi_{z1}}{\mathrm{d}x^2}+\left(\frac{h}{2}\right)^2\frac{\mathrm{d}^2\varphi_{z2}}{\mathrm{d}x^2}+\left(\frac{h}{2}\right)^3\frac{\mathrm{d}^2\varphi_{z3}}{\mathrm{d}x^2}\right)\right]\left(R+\frac{h}{2}\right)\right]$$

## 3. Analytical solution, results and discussion

The analytical solution is proposed as

$$\begin{Bmatrix}(u_0,\varphi_{x1},\varphi_{x2},\varphi_{x3})\\ w_0,\varphi_{z1},\varphi_{z2},\varphi_{z3},\Phi\end{Bmatrix} = \sum_{n=1}^{\infty}\begin{Bmatrix}(U_{0m},\Phi_{x1m},\Phi_{x2m},\Phi_{x3m})cos\lambda_n x\\ (W_{0m},\Phi_{z1m},\Phi_{z2m},\Phi_{z3m},\Phi_m)sin\lambda_n x\end{Bmatrix}, \quad (28)$$

where $U_{0m}$, $W_{0m}$, $\Phi_{xim}$, $\Phi_{zim}$ are the maximum values of the displacements, rotations and electric potential. By definition of amplitude vector $\{X\} = [U_m \ W_m \ \Phi_{x1m} \ \Phi_{z1m} \ \Phi_{x2m} \ \Phi_{z2m} \ \Phi_{x3m} \ \Phi_{z3m}]^T$ and substitution of solution from Eq. (30) into Eq. (29), the solution is reduced to following algebraic equation as

$$[K]\{X\} = \{F\}, \quad (29)$$

Figs. 2 and 3 show variation of $\overline{u_0}$ and $\overline{w_0}$ in terms of $\bar{l} = l/h_T$ for various $\Psi_0$, respectively ($h_T = h + 2h_p$). The numerical results indicate that both axial and radial displacements are decreased with increase of dimensionless micro-length scale parameter. Based on MCST and results of this theory, one can conclude that the stiffness of cylindrical micro-shell is increased with an increase in dimensionless micro length scale parameter. In addition, it is observed that both axial and radial displacements are decreased with an increase in applied electric potentials.

Shown in Figs. 4 and 5 are variation of $\overline{u_0}$ and radi $\overline{w_0}$ in terms of $L/R$ for various $\bar{l}$. It is concluded that an increase in $L/R$ the stiffness of micro-shell is decreased and then the both displacements are increased. In addition, it can be stated that effect of $\bar{l}$ is depending on the values of other geometric parameters. It is concluded that for lower values of $L/R$, increase in $\bar{l}$ leads to an increase in structural stiffness and then a decrease in radial and axial displacements.

Shown in Figs. 6 and 7 are the variation of $\overline{u_0}$ and $\overline{w_0}$ displacements in terms of $K_1, K_2$, respectively. The numerical results indicate that the radial displacement is significantly decreased with an increase in two parameters of Pasternak's foundation. It is concluded that with an increase in two parameters of Pasternak's foundation, the stiffness along the radial direction is increased and then the stiffness along the axial direction is decreased. Based on this conclusion, the axial displacement is increased significantly with increase of both parameters of Pasternak's foundation.

Shown in Figs. 8 and 9 are variation of $\overline{u_0}$ and $\overline{w_0}$ in terms of dimensionless length to radius ratio $L/R$ and $\bar{l}$ of

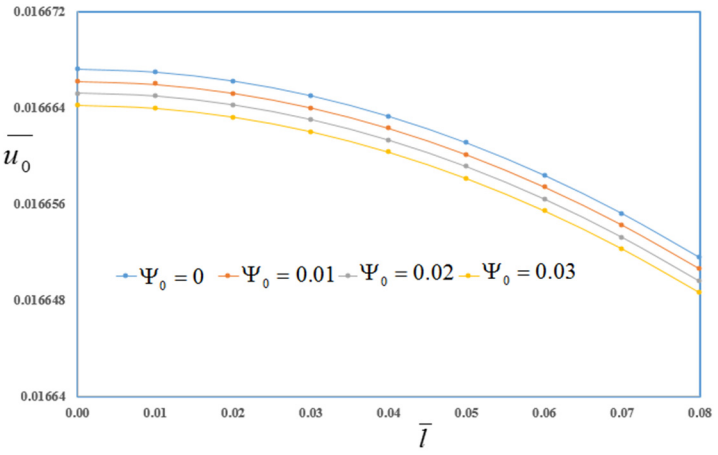


Fig. 2 Variation of $\overline{u_0}$ in terms of $\bar{l}$ for various $\Psi_0$

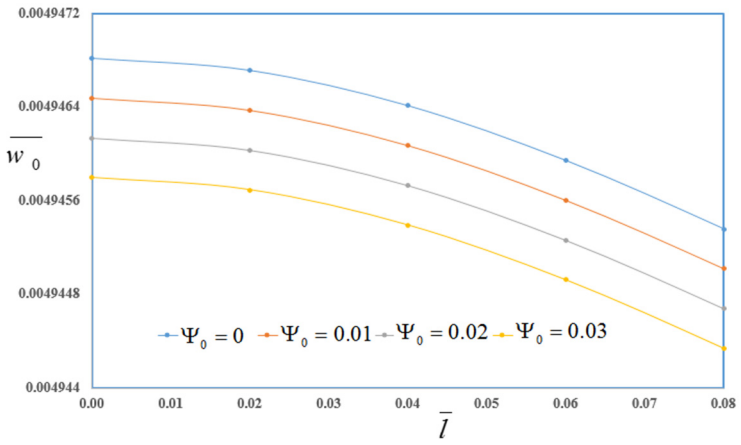


Fig. 3 Variation of $\overline{w_0}$ in terms of $\bar{l}$ for various $\Psi_0$

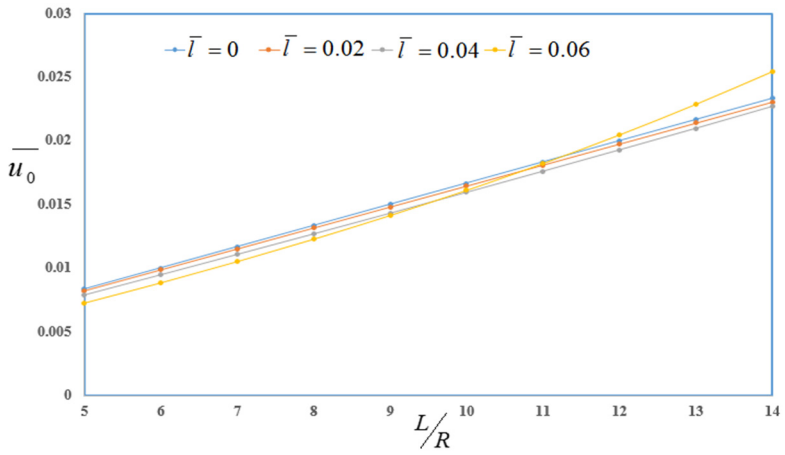


Fig. 4 Variation of $\overline{u_0}$ in terms of $L/R$ for various $\bar{l}$

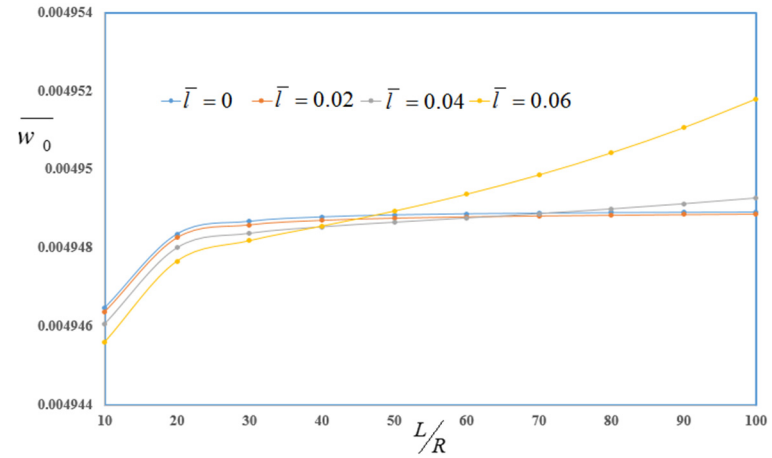


Fig. 5 Variation of $\overline{w_0}$ in terms of $L/R$ for various $\bar{l}$

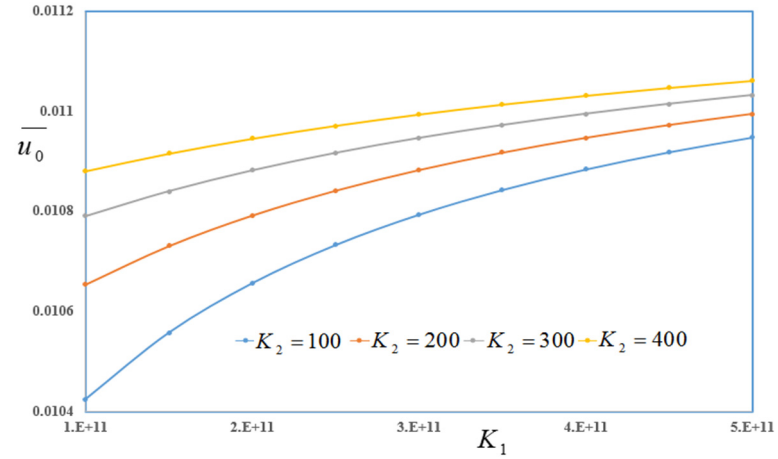


Fig. 6 Variation of $\overline{u_0}$ in terms of $K_1, K_2$

the cylindrical micro-shell. The numerical results indicate that an increase in $L/R$ yields a softer cylindrical shell with an increase in both displacements. In addition, it is observed that for lower values of dimensionless length to radius ratio $L/R$, an increase in dimensionless micro length scale parameter $\bar{l}$ leads to a decrease in radial and axial displacements.

## 4. Conclusions

MCST as well as higher-order shear deformation theory were used in this work for electro-elastic bending analysis of shear deformable three-layered cylindrical micro-shell integrated with piezoelectric layers subjected to mechanical and electrical loads. Size-dependency was included in

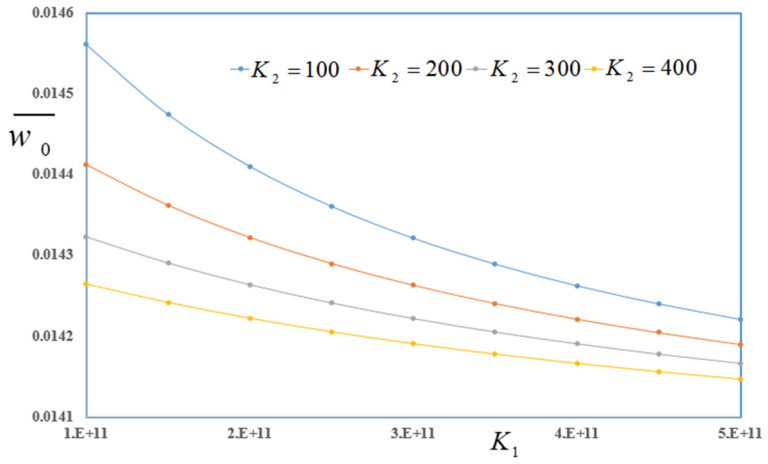


Fig. 7 Variation of $\overline{w_0}$ in terms of $K_1, K_2$

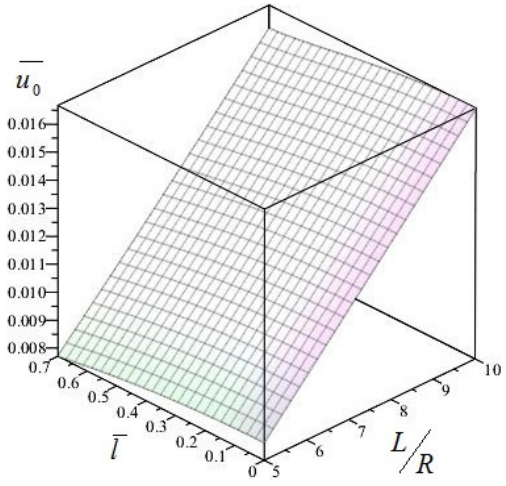


Fig. 8 Variation of $\overline{u_0}$ in terms of $L/R$ and $\bar{l}$

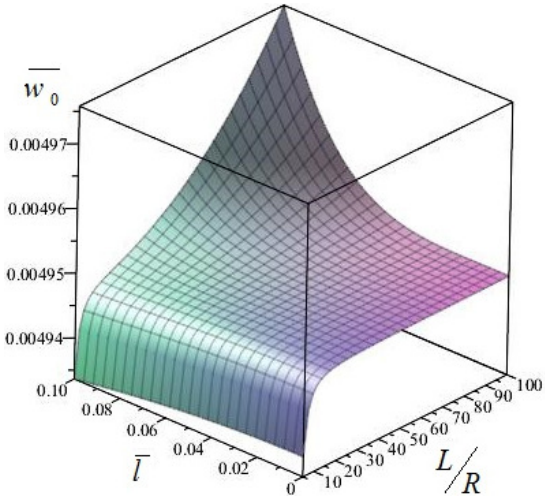


Fig. 9 Variation of $\overline{w_0}$ in terms of $L/R$ and $\bar{l}$

governing equations using MCS including a micro length scale parameter. A two-dimensional electric potential was applied on the piezoelectric layers including a linear variation along thickness direction to account applied electric potential and a longitudinal function to satisfy electrical boundary conditions at both ends of cylindrical shell. The governing equations were derived based on principle of virtual work. Main conclusions of this paper are expressed as:

- Applied electric potential has significant effect on the electro-elastic results of cylindrical microshell. It is concluded that an increase in applied electric potential leads to a decrease in radial and axial displacements.
- Investigation on the effect of micro length scale parameter associated with modified couple stress theory indicates that the radial displacement is decreased with an increase in this length scale parameter. It is concluded that the stiffness of material is increased with an increase in micro length scale parameter.
- Effect of two parameters of the Pasternak's foundation on the radial and axial displacements indicates that an increase in these parameters leads to an increase in stiffness along the radial direction. it is concluded that with an increase in two parameters of Pasternak's foundation, the radial displacements are decreased while the axial displacements are increased.

## References

Abedini, M. and Zhang, C. (2021), "Dynamic vulnerability assessment and damage prediction of RC columns subjected to severe impulsive loading", *Struct. Eng. Mech., Int. J.*, **77**(4), 441-461. https://doi.org/10.12989/sem.2021.77.4.441

Ahmadi, I. and Najafi, M. (2016), "Three-dimensional stresses analysis in rotating thin laminated composite cylindrical shells", *Steel Compos. Struct., Int. J.*, **22**(5), 1193-1214. https://doi.org/10.12989/scs.2016.22.5.1193

Alam, Z., Zhang, C. and Samali, B. (2020a), "Influence of seismic incident angle on response uncertainty and structural performance of tall asymmetric structure", *Struct. Des. Tall Spec. Build.*, **29**(12), e1750. https://doi.org/10.1002/tal.1750

Alam, Z., Zhang, C. and Samali, B. (2020b), "The role of viscoelastic damping on retrofitting seismic performance of asymmetric reinforced concrete structures", *Earthq. Eng. Eng.*

*Vib*., **19**(1), 223-237. https://doi.org/10.1007/s11803-020-0558-x

Anitescu, C., Atroshchenko, E., Alajlan, N. and Rabczuk, T. (2019), "Artificial neural network methods for the solution of second order boundary value problems", *Comput. Mater. Continua*, **59**(1), 345-359. https://doi.org/10.32604/cmc.2019.06641

Arefi, M. (2013), "Nonlinear thermoelastic analysis of thick-walled functionally graded piezoelectric cylinder", *Acta. Mech*., **224**(11), 2771-2783. https://doi.org/10.1007/s00707-013-0888-0

Arefi, M. and Civalek, O. (2020), "Static analysis of functionally graded composite shells on elastic foundations with nonlocal elasticity theory", *Arch. Civil. Mech. Eng*., **20**(1), 1-17. https://doi.org/10.1007/s43452-020-00032-2

Arefi, M. and Rahimi, G.H. (2011a), "Non linear analysis of a functionally graded square plate with two smart layers as sensor and actuator under normal pressure", *Smart Struct. Syst*., *Int. J*., **8**(5), 433-447. https://doi.org/10.12989/sss.2011.8.5.433

Arefi, M. and Rahimi, G.H. (2011b), "Thermo elastic analysis of a functionally graded cylinder under internal pressure using first order shear deformation theory", *Sci. Res. Essays*, **5**(12), 1442-1454. https://doi.org/10.5897/SRE.9000953

Arefi, M. and Rahimi, G.H. (2012a), "Three-dimensional multi-field equations of a functionally graded piezoelectric thick shell with variable thickness, curvature and arbitrary nonhomogeneity", *Acta. Mech*., **223**(1), 63-79. https://doi.org/10.1007/s00707-011-0536-5

Arefi, M. and Rahimi, G.H. (2012b), "Studying the nonlinear behavior of the functionally graded annular plates with piezoelectric layers as a sensor and actuator under normal pressure", *Smart Struct. Syst*., *Int. J*., **9**(2), 127-143. https://doi.org/10.12989/sss.2012.9.2.127

Arefi, M. and Rahimi, G.H. (2012c), "Comprehensive thermoelastic analysis of a functionally graded cylinder with different boundary conditions under internal pressure using first order shear deformation theory", *Mechanika*, **18**(1), 5-13. https://doi.org/10.5755/j01.mech.18.1.1273

Arefi, M. and Zenkour, A.M. (2018), "Size-dependent electro-elastic analysis of a sandwich microbeam based on higher-order sinusoidal shear deformation theory and strain gradient theory", *J. Intel. Mater. Syst. Struct*., **29**(7), 1394-1406. https://doi.org/10.1177/1045389X17733333

Arefi, M. and Zenkour, A.M. (2019), "Influence of magneto-electric environments on size-dependent bending results of three-layer piezomagnetic curved nanobeam based on sinusoidal shear deformation theory", *J. Sandw. Struct. Mater*., **21**(8), 2751-27781. https://doi.org/10.1177/1099636217723186

Arefi, M., Karroubi, R. and Irani-Rahaghi, M. (2016), "Free vibration analysis of functionally graded laminated sandwich cylindrical shells integrated with piezoelectric layer", *Appl. Math. Mech*., **37**(7), 821-834. https://doi.org/10.1007/s10483-016-2098-9

Arefi, M., Mohammadi, M., Tabatabaeian, A., Dimitri, R. and Tornabene, F. (2018), "Two-dimensional thermo-elastic analysis of FG-CNTRC cylindrical pressure vessels", *Steel Compos. Struct*., *Int. J*., **27**(4), 525-536. https://doi.org/10.12989/scs.2018.27.4.525

Arefi, M., Moghaddam, S.K., Bidgoli, E.M.R., Kiani, M. and Civalek, O. (2021), "Analysis of graphene nanoplatelet reinforced cylindrical shell subjected to thermo-mechanical loads", *Compos. Struct*., **255**(1), 112924. https://doi.org/10.1016/j.compstruct.2020.112924

Areias, P. and Rabczuk, T. (2013), "Finite strain fracture of plates and shells with configurational forces and edge rotations", *Int. J. Num. Meth. Eng*., **94**(12), 1099-1122. https://doi.org/10.1002/nme.4477

Areias, P., Rabczuk, T. and Msekhdc, M.A. (2016), "Phase-field analysis of finite-strain plates and shells including element subdivision", *Comput. Methods. Appl. Mech. Eng*., **312**, 322-350. https://doi.org/10.1016/j.cma.2016.01.020

Beni, Y.T., Mehralian, F. and Razavi, H. (2015), "Free vibration analysis of size-dependent shear deformable functionally graded cylindrical shell on the basis of modified couple stress theory", *Compos. Struct*., **120**, 65-78. https://doi.org/10.1016/j.compstruct.2014.09.065

Chakraborty, S., Dey, T. and Kumar, R. (2019), "Stability and vibration analysis of CNT-Reinforced functionally graded laminated composite cylindrical shell panels using semi-analytical approach", *Compos. B: Eng*., **168**, 1-14. https://doi.org/10.1016/j.compositesb.2018.12.051

Chao, M., Kai, C. and Zhiwei, Z. (2020), "Research on tobacco foreign body detection device based on machine vision", *Trans. Inst. Measur. Cont*., **42**(15), 2857-2871. https://doi.org/10.1177/0142331220929816

Dehsaraji, M.L., Arefi, M. and Loghman, A. (2020), "Three dimensional free vibration analysis of functionally graded nano cylindrical shell considering thickness stretching effect", *Steel Compos. Struct*., *Int. J*., **34**(5), 657-680. http://dx.doi.org/10.12989/scs.2020.34.5.657

Duan, Z., Li, C., Ding, W., Zhang, Y., Yang, M., Gao, T., Cao, H., Xu, X., Wang, D., Mao, C. and Li, H.N. (2021), "Milling force model for aviation aluminum alloy: Academic insight and perspective analysis", *China J. Mech. Eng*., **34**(1), 1-35. https://doi.org/10.1186/s10033-021-00536-9

Ebrahimi, F., Daman, M. and Jafari, A. (2017), "Nonlocal strain gradient-based vibration analysis of embedded curved porous piezoelectric nano-beams in thermal environment", *Smart Struct. Syst*., *Int. J*., **20**(6), 709-728. https://doi.org/10.12989/sss.2017.20.6.709

Gholami, R., Darvizeh, A., Ansari, R. and Hosseinzadeh, M. (2014), "Size-dependent axial buckling analysis of functionally graded circular cylindrical microshells based on the modified strain gradient elasticity theory", *Meccanica*, **49**(7), 1679-1695. https://doi.org/10.1007/s11012-014-9944-7

Guo, H., Zhuang, X. and Rabczuk, T. (2019), "A deep collocation method for the bending analysis of Kirchhoff plate", *Comput. Mater. Continua*., **59**(2), 433-456. https://doi.org/10.32604/cmc.2019.06660

Haldar, S., Majumder, A. and Kalita, K. (2019), "Bending analysis of composite skew cylindrical shell panel", *Struct. Eng. Mech*., *Int. J*., **70**(1), 125-131. https://doi.org/10.12989/sem.2019.70.1.125

Huang, B., Li, C., Zhang, Y., Ding, W., Yang, M., Yang, Y., Zhai, H., Xu, X., Wang, D., Debnath, S., Jamil, M., Li, H.N., Ali, H.M., Gupta, M.K. and Said, Z. (2021), "Advances in fabrication of ceramic corundum abrasives based on sol–gel process", *China J. Aeron*., **34**(6), 1-17. https://doi.org/10.1016/j.cja.2020.07.004

Javed, S., Viswanathan, K.K. and Aziz, Z.A. (2016), "Free vibration analysis of composite cylindrical shells with non-uniform thickness walls", *Steel Compos. Struct*., *Int. J*., **20**(5), 1087-1102. https://doi.org/10.12989/scs.2016.20.5.1087

Ke, L.L., Wang, Y.S. and Reddy, J.N. (2014a), "Thermo-electro-mechanical vibration of size-dependent piezoelectric cylindrical nanoshells under various boundary conditions", *Compos. Struct*., **16**, 626-636. https://doi.org/10.1016/j.compstruct.2014.05.048

Ke, L.L., Wang, Y.S., Yang, J. and Kitipornchai, S. (2014b), "The size-dependent vibration of embedded magneto-electro-elastic cylindrical nanoshells", *Smart. Mater. Struct*., **23**, 125036. https://doi.org/10.1088/0964-1726/23/12/125036

Khoshgoftar, M.J., Rahimi, G.H. and Arefi, M. (2013), "Exact solution of functionally graded thick cylinder with finite length under longitudinally non-uniform pressure", *Mech. Res. Commun*., **51**, 61-66.

https://doi.org/10.1016/j.mechrescom.2013.05.001

Lal, A., Saidane, N. and Singh, B.N. (2012), "Stochastic hygrothermoelectromechanical loaded post buckling analysis of piezoelectric laminated cylindrical shell panel", *Smart Struct. Syst*., *Int. J*., **9**(6), 505-534. https://doi.org/10.12989/sss.2012.9.6.505

Lei, Z. and Tong, L. (2019), "Semi-analytical solutions of free and force vibration behaviors of GRC-FG cylindrical shells", *Steel Compos. Struct*., *Int. J*., **32**(5), 687-699. https://doi.org/10.12989/scs.2019.32.5.687

Li, H., Pang, F., Du, Y. and Gao, C. (2019), "Free vibration analysis of uniform and stepped functionally graded circular cylindrical shells", *Steel Compos. Struct*., *Int. J*., **33**(2), 163-180. https://doi.org/10.12989/scs.2019.33.2.163

Li, C., Sun, L., Xu, Z., Wu, X., Liang, T. and Shi, W. (2020), "Experimental investigation and error analysis of high precision FBG displacement sensor for structural health monitoring", *Int. J. Struct. Stab. Dyn*., **20**(06), 2040011. https://doi.org/10.1142/S0219455420400118

Liu, J., Yi, Y. and Wang, X. (2020), "Exploring factors influencing construction waste reduction: A structural equation modeling approach", *J. Clean. Prod*., **276**, 123185. https://doi.org/10.1016/j.jclepro.2020.123185

Liu, M., Li, C., Cao, C., Wang, L., Li, X., Che, J., Yang, H., Zhang, X., Zhao, H., He, G. and Liu, X. (2021), "Walnut fruit processing equipment: academic insights and perspectives", *Food Eng. Rev*., 1-36. https://doi.org/10.1007/s12393-020-09273-6

Mehralian, F., Beni, Y.T. and Ansari, R. (2016a), "On the size dependent buckling of anisotropic piezoelectric cylindrical shells under combined axial compression and lateral pressure", *Int. J. Mech. Sci*., **119**, 155-169. https://doi.org/10.1016/j.ijmecsci.2016.10.006

Mehralian, F., Beni, Y.T. and Ansari, R. (2016b), "Size dependent buckling analysis of functionally graded piezoelectric cylindrical nanoshell", *Compos. Struct*., **152**, 45-61. https://doi.org/10.1016/j.compstruct.2016.05.024

Nanthakumar, S.S., Lahmer, T., Zhuang, X., Zi, G. and Rabczuk, T. (2016), "Detection of material interfaces using a regularized level set method in piezoelectric structures", *Inverse. Prob. Sci. Eng*., **24**(1), 153-176. https://doi.org/10.1080/17415977.2015.1017485

Nguyen-Thanh, N., Zhou, K., Zhuang, X., Areias, P., Nguyen-Xuan, H., Bazilevs, Y. and Rabczuk, T. (2017), "Isogeometric analysis of large-deformation thin shells using RHT-splines for multiple-patch coupling", *Comput. Methods. Appl. Mech. Eng*., **316**, 1157-1178. https://doi.org/10.1016/j.cma.2016.12.002

Rabczuk, T., Ren, H. and Zhuang, X. (2019), "A nonlocal operator method for partial differential equations with application to electromagnetic waveguide problem", *Comput. Mater. Continua*., **59**(1), 31-55. https://doi.org/10.32604/cmc.2019.04567

Razavi, H., Babadi, A.F. and Beni, Y.T. (2017), "Free vibration analysis of functionally graded piezoelectric cylindrical nanoshell based on consistent couple stress theory", *Compos. Struct*., **160**, 1299-1309. https://doi.org/10.1016/j.compstruct.2016.10.056

Rouhi, H., Ansari, R. and Darvizeh, M. (2016), "Nonlinear free vibration analysis of cylindrical nanoshells based on the Ru model accounting for surface stress effect", *Int. J. Mech. Sci*., **113**, 1-9. https://doi.org/10.1016/j.ijmecsci.2016.04.004

Sahmani, S., Aghdam, M.M. and Akbarzadeh, A.H. (2016), "Size-dependent buckling and postbuckling behavior of piezoelectric cylindrical nanoshells subjected to compression and electrical load", *Mater. Des*., **105**, 341-351. https://doi.org/10.1016/j.matdes.2016.05.065

Salehipour, H., Shahsavar, A. and Civalek, O. (2019), "Free vibration and static deflection analysis of functionally graded and porous micro/nanoshells with clamped and simply supported edges", *Compos. Struct*., **221**, 110842. https://doi.org/10.1016/j.compstruct.2019.04.014

Shokrollahi, H. (2018), "Deformation and stress analysis of a sandwich cylindrical shell using HDQ Method", *Steel Compos. Struct*., *Int. J*., **27**(1), 35-48. https://doi.org/10.12989/scs.2018.27.1.035

Sun, J., Wang, Z., Zhou, Z., Xu, X. and Lim, C.W. (2018) "Surface effects on the buckling behaviors of piezoelectric cylindrical nanoshells using nonlocal continuum model", *Appl. Math. Modell*., **59**, 341-356. https://doi.org/10.1016/j.apm.2018.01.032

Sun, L., Yang, Z., Jin, Q. and Yan, W. (2020), "Effect of axial compression ratio on seismic behavior of GFRP reinforced concrete columns", *Int. J. Struct. Stab. Dyn*., **20**(06), 2040004. https://doi.org/10.1142/S0219455420400040

Tadi Beni, Y., Mehralian, F. and Zeighampour, H. (2016), "The modified couple stress functionally graded cylindrical thin shell formulation", *Mech. Adv. Mater. Struct*., **23**(7), 791-801. https://doi.org/10.1080/15376494.2015.1029167

Tohidi, H., Hosseini-Hashemi, S.H. and Maghsoudpour, A. (2018), "Size-dependent forced vibration response of embedded micro cylindrical shells reinforced with agglomerated CNTs using strain gradient theory", *Smart Struct. Syst*., *Int. J*., **22**(5), 527-546. https://doi.org/10.12989/sss.2018.22.5.527

Vu-Bac, N., Lahmer, T., Zhuang, X., Nguyen-Thoi, T. and Rabczuk, T. (2016), "A software framework for probabilistic sensitivity analysis for computationally expensive models", *Adv. Eng. Software*., **100**, 19-31. https://doi.org/10.1016/j.advengsoft.2016.06.005

Wang, Q. and Varadan, V.K. (2007), "Application of nonlocal elastic shell theory in wave propagation analysis of carbon nanotubes", *Smart. Mater. Struct*., **16**, 178. https://doi.org/10.1088/0964-1726/16/1/022

Wang, Y., Li, C., Zhang, Y., Yang, M., Li, B., Jia, D., Hou, Y. and Mao, C. (2016), "Experimental evaluation of the lubrication properties of the wheel/workpiece interface in minimum quantity lubrication (MQL) grinding using different types of vegetable oils", *J. Clean. Prod*., **127**, 487-499. https://doi.org/10.1016/j.jclepro.2016.03.121

Wang, Y., Xie, K., Fu, T. and Zhang, W. (2020), "A unified modified couple stress model for size-dependent free vibrations of FG cylindrical microshells based on high-order shear deformation theory", *Eur. Phys. J. Plus*, **135**, 71. https://doi.org/10.1140/epjp/s13360-019-00012-3

Yang, M., Li, C., Zhang, Y., Jia, D., Zhang, X., Hou, Y., Li, R. and Wang, J. (2017), "Maximum unreformed equivalent chip thickness for ductile-brittle transition of zirconia ceramics under different lubrication conditions", *Int. J. Mach. Tool. Manuf*., **122**, 55-65. https://doi.org/10.1016/j.ijmachtools.2017.06.003

Yeh, J.-Y. (2016), "Vibration characteristic analysis of sandwich cylindrical shells with MR elastomer", *Smart Struct. Syst*., *Int. J*., **18**(2), 233-247. https://doi.org/10.12989/sss.2016.18.2.233

Yin, Q., Li, C., Dong, L., Bai, X., Zhang, Y., Yang, M., Jia, D., Li, R. and Liu, Z. (2021), "Effects of physicochemical properties of different base oils on friction coefficient and surface roughness in MQL milling AISI 1045", *Int. J. Prec. Eng. Manufact-Green Tech*., 1-19. https://doi.org/10.1007/s40684-021-00318-7

Zhang, C. and Wang, H. (2019), "Swing vibration control of suspended structure using active rotary inertia driver system: Parametric analysis and experimental verification", *Appl. Sci*., **9**(15), 3144. https://doi.org/10.3390/app9153144

Zhang, B., He, Y., Liu, D., Shen, L. and Lei, J. (2015), "Free vibration analysis of four-unknown shear deformable functionally graded cylindrical microshells based on the strain gradient elasticity theory", *Compos. Struct*., **119**, 578-597. https://doi.org/10.1016/j.compstruct.2014.09.032

Zhang, Y., Li, C., Ji, H., Yang, X., Yang, M., Jia, D., Zhang, X., Li, R. and Wang, J. (2017), "Analysis of grinding mechanics and improved predictive force model based on material-removal and plastic-stacking mechanisms", *Int. J. Mach. Tool. Manufact.*, **122**, 81-97. https://doi.org/10.1016/j.ijmachtools.2017.06.002

Zhang, C., Alam, Z., Sun, L., Su, Z. and Samali, B. (2019), "Fiber Bragg grating sensor-based damage response monitoring of an asymmetric reinforced concrete shear wall structure subjected to progressive seismic loads", *Struct. Cont. Heal. Monitor.*, **26**(3), e2307. https://doi.org/10.1002/stc.2307

Zhang, J., Wang, M., Tang, Y., Ding, Q., Wang, C., Huang, X., Chen, D. and Yan, F. (2021), "Angular velocity measurement with improved scale factor based on a wideband-tunable optoelectronic oscillator", *IEEE Trans. Instrument. Measur.*, **70**, 1-9. https://doi.org/10.1109/TIM.2021.3067183

Zhao, X., Zhu, W.D. and Li, Y.H. (2020), "Analytical solutions of nonlocal coupled thermoelastic forced vibrations of micro-/nano-beams by means of Green's functions", *J. Sound Vib.*, **481**, 115407. https://doi.org/10.1016/j.jsv.2020.115407

Zuo, C., Chen, Q., Tian, L., Waller, L. and Asundi, A. (2015), "Transport of intensity phase retrieval and computational imaging for partially coherent fields: The phase space perspective", *Opt. Las. Eng.*, **71**, 20-32. https://doi.org/10.1016/j.optlaseng.2015.03.006

Zuo, C., Sun, J., Li, J., Zhang, J., Asundi, A. and Chen, Q. (2017), "High-resolution transport-of-intensity quantitative phase microscopy with annular illumination", *Sci. Rep.*, **7**(1), 1-22. https://doi.org/10.1038/s41598-017-06837-1

*CC*